

International Conference on Space Optics—ICSO 2006

Noordwijk, Netherlands

27–30 June 2006

Edited by Errico Armandillo, Josiane Costeraste, and Nikos Karafolas



Reflective baffle for BepiColombo mission

E. Rugi-Grond, T. Weigel, A. Herren, M. Dominguez Calvo, et al.



REFLECTIVE BAFFLE FOR BEPICOLOMBO MISSION

E. Rugi-Grond⁽¹⁾, T. Weigel⁽¹⁾, A. Herren⁽¹⁾, M Domínguez Calvo⁽¹⁾, U. Krähenbühl⁽¹⁾
D. Mouricaud⁽²⁾, H. Vayssade⁽²⁾

⁽¹⁾Contraves Space AG, Schaffhauserstr. 580, 8052 Zürich Switzerland, Email: elisabetta.rugi@unaxis.com

⁽²⁾SAGEM Défense Sécurité 91280 Saint-Pierre du Perray, France, Email: herve.vayssade@sagem.com

ABSTRACT

The BepiColombo Spacecraft can't tolerate to absorb a major fraction of the off-axis sunlight through larger payload apertures. Fortunately, there are solutions to design baffles such that they reflect the incoming radiation back through the front aperture rather than absorbing it. A Design Study, sponsored by ESA and performed by Contraves Space together with SAGEM Défense Sécurité, has analysed the potential of various solutions and assessed the options to manufacture them. The selected configuration has been analysed in detail for the optical, mechanical and thermal performance as well as the impact on mass and power dissipation. The size of the baffle was adapted to the needs of the BepiColombo Laser Altimeter (BELA) payload.

1. WHY A REFLECTIVE BAFFLE

Initially, reflective baffles have been invented to protect cold infrared telescopes and payloads. The motivation is comparable with a mission to Mercury: Need for baffling under severe thermal constraints.

The solar irradiance at planet Mercury is as much as 11 times stronger compared to Earth environment. The recently launched NASA S/C MESSENGER has a huge sunshade which keeps the whole payload module always in the shadow. But this constrains S/C pointing, and the payload will most of the time not look towards Nadir. BepiColombo is free of that constraint and can provide Nadir-pointing. That's great for payloads like the Laser Altimeter, but what about these 400 W solar power which in turn may pass through the 250 mm¹ large front aperture? Optical filters may suppress most of the solar and thermal infrared power. Typical passive optical payloads would still receive sufficient signal because of the illumination on the Mercury surface is brighter at the same scale. But active optical payloads, with an internal light source like the Laser Altimeter, would loose 30-50% system transmission in two passes and further drive up the needs for laser power and receiver aperture size. Moreover, what if this large window would break? Failure of that component would let collapse the whole S/C

¹ The BELA receiver aperture was meanwhile reduced to 200 mm.

thermal control concept. Deep concerns would be raised to that component, resulting in comfortable margins of safety and eventually a mass impact in the order of 1-1.3 Kg.

If instead a baffle could be designed such that it reflects off most of the received power, there would be no further transmission loss. The failure mode would rather consist in a graceful degradation. Sure, a baffle would have a mass of ~1.5 Kg too. But mass and power is saved through the smaller sizing of the Laser Altimeter behind.

2. REQUIREMENTS

The following requirements were given to the Design Study.

Table 1: Requirements given to the Study

Optical Requirements	
Payload Clear Aperture	250 mm
Payload Field of View	350 μrad
Aspect Angle	35°
Rejection efficiency	>95%
Straylight $\Phi_{\text{exit}}/\Phi_{\text{entrance}}$	<10 ⁻³
Mechanical Requirements	
Envelope Diameter	<300 mm
Envelope Length	<550 mm
Mass	<1.5 Kg
Eigenfrequency	>100 Hz
Thermal Requirements	
Case 1:	T _{max} <80°C
Case 2:	no constraint

3. HOW A REFLECTIVE BAFFLE WORKS

Some sort of optics will be needed to do that. But other than telescopes and cameras, which perform a point-to-point imaging, it is sufficient to direct the light towards or away from specific zones. The concepts are found in illumination design, sometimes called "Non-imaging Optics" [6].

Let us consider an ellipse (Fig 1). A ray (1), which passes through one focus and being reflected, will pass through the other focus. That's not all. Rays (2) passing between the two focal points and being reflected

will pass again between the two. That leads to a basic idea: Let's wrap the two focal points around the entrance aperture.

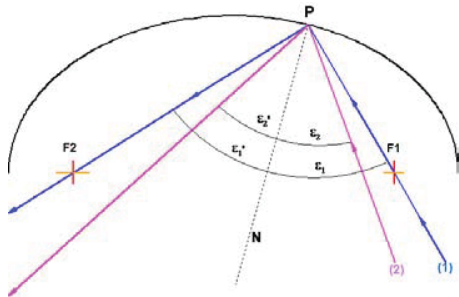


Fig. 1: Rays reflected at an elliptical curve

In order not to obscure the payload field of view, several ellipses are stacked over each other (Figure 2).

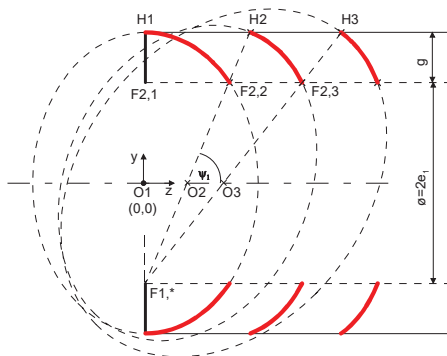


Fig 2: Elliptical sections stacked over each other.

The arrangement was invented by Danilo Radovich in 1978 [1], further mentioned in [2], [3]. The first ellipse is placed with their focal points $F_{1,1}$ and $F_{2,1}$ at the entrance edge, the vertex points $H1$ form the outer bound. The second ellipse is placed such that the first focus $F_{1,2}$ stays at the entrance together with $F_{1,1}$. The second focus $F_{2,2}$ is placed at the inner tip of the previous ellipse. The remaining degree of freedom is used to place the vertex point H_2 at the outer bound of the baffle. The physical surfaces are not Ellipsoids. They result from the revolution of the elliptical curves around the optical axis z .

The incoming rays go off with only one reflection. However, the considerations so far work fine in the plane of paper, but not as perfect when going to 3D space. Some skew rays miss to pass back through the previous apertures and hit the rear sides of the previous segments. In order to protect for stray light, the rear surfaces would need to be diffuse black. Up to ~10 % of the rays would be trapped.

The study performed several attempts either to open the gaps sideward or to close them by adding rear facing reflective spherical segments. The ray efficiency could be brought up to ~98%. However, many reflections take place then, and the overall power efficiency

stays 90-92%. Moreover, 0.2-0.4% of the incoming power may reach the exit in specular reflection.

The most elegant solution to avoid the cavities was found by Stavroudis [4] with the use of hyperbolas (Fig. 3 and Fig. 4).

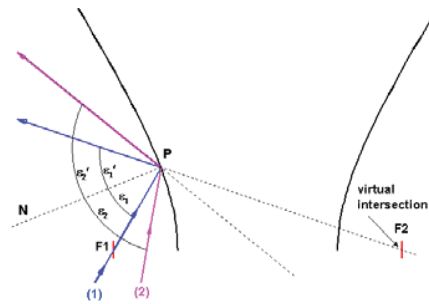


Fig 3: Hyperbolas: A ray (1) passes focal point F_1 , but can not reach focal point F_2 . However, its direction appears as it would come from F_2 . A ray (2) passing between the focal points and being reflected, keeps at least the trajectory between the focal points.

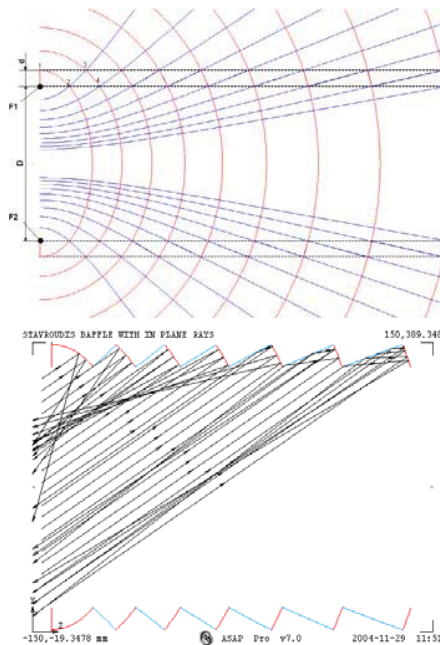


Fig 4: A sequence of **ellipses** and **hyperbolas**, alternating between outer and inner diameter, forms the Stavroudis baffle.

While ellipses form from the outer to the inner diameter along the axis of symmetry, the hyperbolas do the opposite (Figure 4). By means of connecting the ellipses with hyperbolas, we obtain a continuous cylinder without cavities. All two focal points of all segments stay at the entrance edge.

The concept accepts that rays, which fall first onto a hyperbola, will need a second reflection on an ellipse. But it works also in 3D space out of plane. Some skew rays need more than 2 reflections, but all go out. It is

further expected that this concept is more tolerant against shape distortions [5] compared with the Radovich one. However, the rear facing hyperbolas cause more stringent requirements on surface finish.

The two concepts presented so far have a rather complex shape. There are more simple solutions. The Compound Parabolic Concentrator CPC [6] concentrates all light arriving within a certain solid angle onto a specific aperture. Inversely, all light arriving outside that angle is kept away from that aperture. (Figure 5)

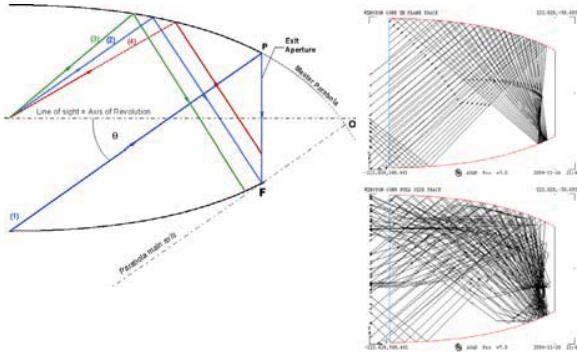


Fig. 5: Compound Parabolic Concentrator – left the principle – right up rays in plane – right down full beam

The design is completely determined with the aspect angle and the exit diameter. For BELA, it results to a front diameter of 436 mm and a length of 490 mm, more than the Radovich and Stavroudis concepts. Not only would the mass increase. The 1.74 times larger front diameter would collect 3 times more power. Together with the 3-4 reflections needed, this baffle would absorb ~6-7 times more power. On the other hand, the baffle has a large solid angle for off-radiation, because all internally reflected thermal power will be sent off through the front.

The Compound Elliptic Concentrator CEC [6],[8] provides more design flexibility. It is equivalent to the CPC, but dedicated to light sources at finite distance. The study has investigated its potential to reduce the front diameter and make it equal to the BELA aperture. However, for the required aspect angle of 35° the baffle would result in a length of 1.2m. With a length constraint of 550 mm, design solutions are only obtained for aspect angles >55°. Using both the constraints in length and angle, the computer optimization attempts to shift the second focus to infinity and eventually results to a Parabola.

The design by William Linlor [9] (Fig. 6), intended for the SIRTF/ Spitzer Space Telescope, foresees spherical and straight pairs of surfaces. The light bends around

between them back into the incoming direction. That needs many reflections and performs well only for thermal infrared power.

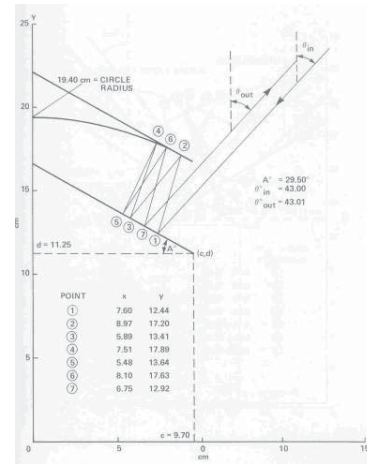


Fig. 6: The Linlor Concept

4. TRADE-OFF

Eight configurations in total have undergone the trade-off. The best solutions have been found with a somewhat modified Radovich configuration and the Stavroudis baffle manufactured in several pieces. The result arises primarily from the low number of reflections needed. Final preference was given to the Stavroudis baffle, because it was considered the more robust solution.

It shall be mentioned that the CPC loses terrain because of its increased entrance. That disadvantage would not exist if a payload with a field of view of 10° would be considered. A second trade-off on a fictitious camera showed that the CPC would become competitive because of its easy shape. But it must not be forgotten that the CPC would become a concentrator if the sun should arrive by accident at angles <35°. It also concentrates the Planetary thermal power <35°.

5. OPTICAL DESIGN DEFINITION

The optical design is completely determined with the definition of the inner and outer diameter, the payload field of view and a length constraint. The minimum aspect angle of 35° results into a minimum length of 361 mm. Although the overall length constraint was given with 550 mm, there was no room to use that because of the mass constraint. With the inner diameter given, the outer diameter was iterated such that the resulting length just meets the minimum aspect angle.

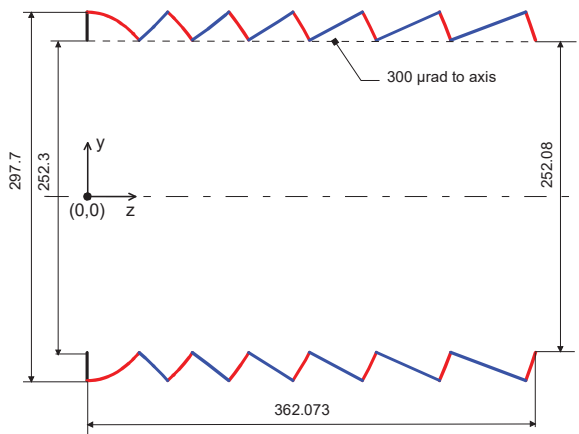


Fig. 7: Dimensions of the baffle

6. MANUFACTURING ASPECTS

6.1 Baffle Structure

The study has investigated four principal options to manufacture the baffle structure:

1. Electroforming on a plastic mandrel.
2. Diamond turning in one or several pieces
3. Filament Winding
4. Fine casting.

In terms of geometry, the first two have the best chance to meet the accuracy.

Electroforming promises the best surface finish (XMM: <1nm) and the smallest wall thickness. In turn, the choice of material is limited to Nickel, Nickel Alloys and Copper, all having a relative high specific density. Aluminium can not be electroformed. Thus the mass saving by small thickness is mitigated. On the other hand, thermal aspects require sufficient cross section for thermal conduction. There are recent experiences at Media Lario with electroforming of Magnesium. It is however too early to assess the technical and programmatic impact of that option. The economical advantage, i.e. making several pieces from one mandrel, does not exist here as the mandrel needs to be dissolved and destroyed for separation.

Diamond turning offers a wider range of materials. The surface finish— without polishing - can reach ~5nm, but not over the full length. The baffle must be made in several pieces and assembled afterwards.

Trade-Off: When comparing the first two options, the only winning aspect of Electroforming is the surface finish. Diamond turning wins in all other aspects including mass because of the choice of Aluminium more than compensates the larger thickness, providing better thermal conduction at the same time. Diamond turning has also advantages in programmatic aspects like the design flexibility.

Filament Winding and Fine Casting are not suitable for the complexity of the shape.

The trade-off selected diamond turning as baseline.

5.2 Interior Coating

With the baffle geometry chosen, the final rejection performance depends to much extend on the surface reflectivity. Taking into account the large spectral range over the solar spectrum and the thermal infrared radiation of the planet, only two metallic coatings provide sufficient reflectivity: Silver (94.5% in solar spectrum) and Aluminium (91% in solar spectrum). The reflectivity of silver is actually >97% in most of the spectrum, but is much reduced in the ultraviolet part. There are solutions to enhance that dip by means of dielectric overcoats.

Unfortunately, Silver is a chemical instable material. It tends to oxidization and has affinity to sulphur.

The feasibility of a silver coating on this kind of baffle has been studied at SAGEM Défense Sécurité (the former REOSC). SAGEM suggested 3 coatings out of their heritage:

1. A standard Protected Silver coating.
2. A space qualified Protected Silver coating, used on the Heat Dump Mirror (HDM) of the Japanese Solar-B Space Telescope.
3. An Enhanced Silver coating developed for the Southern Africa Large (ground) Telescope SALT

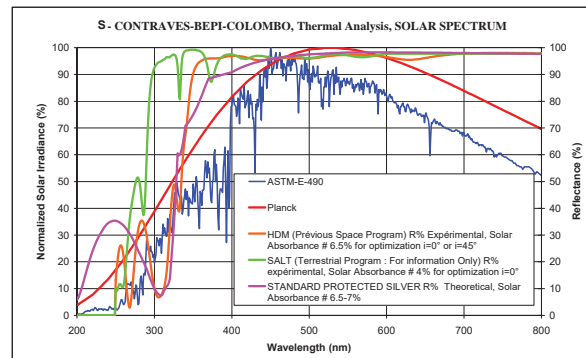


Fig 8: The reflectivity of the three silver coatings in comparison with the solar spectrum (blue: ASTM E-490, red: Planck spectrum).

The green curve for SALT shows the ultraviolet amplification, which achieves an overall reflectivity in the solar spectrum of 96.8 %. This value is sensitive to the angle of incidence and to the achieved thickness tolerances of the dielectric layers on top. The homogeneity of the layer thickness suffers from the surface curvatures. There are measures like masking to take control about the deposition. Breadboarding is eventually needed to get confidence about the achievable performance on the baffle segments.

The coating features also some degradation in the thermal infrared due to absorption of the oxide layers:

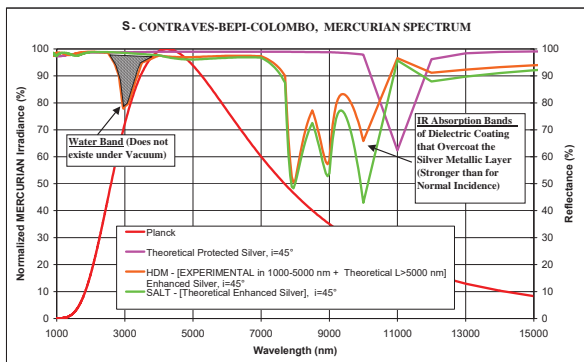


Fig. 9: Reflectivity in the Thermal IR spectrum.

The silver coating causes further implications:

- The Nickel adhesion layer constrains the upper temperature to 150°C. Above that, Nickel delamination takes place.
- The edge radius of the inner vane tips will not be better than 0.1 mm.

Due to technological constrains, different types of coating might be necessary for the front and rear facing sides of one segment.

7. BAFFLE DESIGN AND MECHANICAL PROPERTIES

For the purpose of this study, the mechanical and thermal functions were kept separate:

- The baffle support structure carries only the mechanical loads.
- Thermal control is solely performed by means of Thermal Hardware (straps)

The baffle cylinder is composed of three pieces.

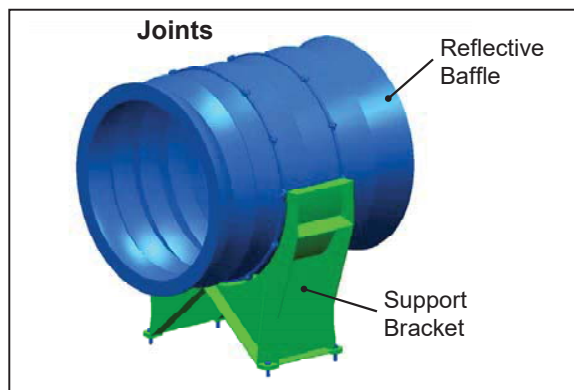


Fig. 10: Mechanical Design of the baffle

Mass and Dimensions result to:

Table 2: Baffle Design Data

Baffle Cylinder	
Insider Diameter	252.3 mm
Outside Diameter	298.7 mm
Length	362.1 mm
Wall thickness	0.5 mm
Number of segments	3
Mass	780 g
Material	Aluminium
Support Bracket	
Material	Aluminium
Wall thickness	1 mm
Mass	580 g
Total Mass Baffle + Bracket:	1.36 Kg

For the purpose of joining the segments, the use of bolts, adhesives, or welding/brazing/soldering techniques are foreseen.

The response to mechanical loads results to:

Table 3: Response to mechanical loads

Eigenfrequencies		
1. mode		167 Hz
2. mode		224 Hz
3. mode		258 Hz
Launch Loads, acceleration 64.4 g		
X	Von Mises Stresses	22.7 MPa
	Buckling Load Factor	22
Y	Von Mises Stresses	24.7 MPa
	Buckling Load Factor	23.4
Z	Von Mises Stresses	11.9 MPa
	Buckling Load Factor	55.9

The Eigenfrequencies result comfortably higher than required. Also the stresses stay well below the critical levels, and there are no buckling problems. Unfortunately, no mass saving potential is gained from this result as the baffle wall thickness is rather determined from the need of thermal conductivity and manufacturing aspects.

8. THERMAL PERFORMANCE

The thermal performance has been analysed at three Mercury seasons: Perihelion, 60° from Perihelion (no eclipse anymore from the planet) and 120° (Fig. 11):

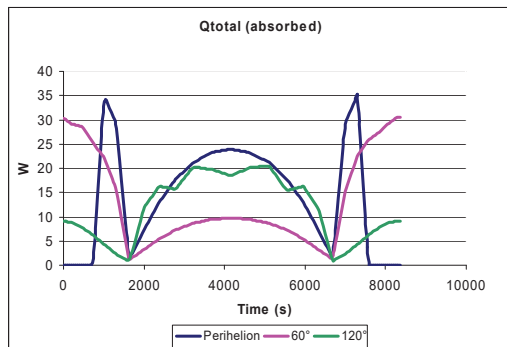


Fig 11: Flux absorbed in the 3 seasons

Three thermal control configurations have been analysed:

- Thermal Equilibrium with only radiative coupling to space. No thermal flux goes into the spacecraft.
- Thermal equilibrium only via radiative couplings with the baffle isolated from the S/C by MLI.
- Thermal equilibrium via radiative couplings with the baffle isolated from the radiative S/C environment by MLI and conductive couplings to a dedicated S/C radiator.

The thermal control measures were:

- MLI wrapped around the external baffle surface for insulation with the S/C thermal environment (60°C)
- Copper straps to the S/C radiator (60°C), with 100 mm length and equivalent cross section of $5 \times 2 \text{ mm}^2$

Table 4: Analysis Results for Perihelion Season

	Average Temp. °C	Flux to SC, W	Thermal HW mass
A	220-225	0	
B	110-140	Rad: 6-12, ave 6	
C1	90-125	Rad 3.5-9.5, ave 6.4 Cond: 2-7, ave 3.7	200 g
C2	65-81	Rad: 1-3, ave 2 Cond: 1.75-15, ave 8	1400g

Rad: Radiative coupling; cond: conductive coupling

The uncoupled configuration A) reaches temperatures above the limit what the coating could withstand. The radiative coupled configuration B) has the average temperature below the critical limit, but still has critical hot areas in the rear part (170°). It shows axial gradients up to 110 K and radial gradients up to 90 K. From opto-mechanical analysis it is known that 30-40K can be tolerated in radial direction without performance degradation. There are further hot spots in the first 3 segments. With 200g thermal hardware spent there, the gradients are reduced to 35K radial and 80K longitudinal, but the average temperature is still above 100°C.

In order to get down to 80°C, 1400g would need to be spent, now including also the last four segments. The actual thermal hardware needed to reduce the baffle temperature depends on the value to be reached.



Figure 12: Strap configuration

When going to the uneclipsed case at 60° argument of Perihelion, with the last strap configuration, the average temperature further increases to 90°C, and further hot spots of 200°C show up in the front segments.

An improvement with no additional straps may be obtained by making the outer surface of the baffle black. That would get the average temperature down to 60-68°C and the peak temperatures to 100°C. In both cases (black or not) the average flux to the S/C stays ~10 W, almost the same as at Perihelion season.

The 120° argument of perihelion season resulted less critical.

9. OPTICAL PERFORMANCE

9.1 Power Rejection Performance

A surface reflectivity of 96.8 % (SALT coating) has been assumed. The degradation due to angular variations, contaminations and scatter is assumed to result in a reflectivity 95% in the solar spectrum. The TIR reflectivity will be ~93.5 %. The overall rejection performance of the baffle results with

- 93-94% in the solar spectrum
- 91-92% in the thermal infrared spectrum

The variation is due to the angle of incidence and the resulting number of reflections. It is worst between 60-70° and best above 80° from the optical axis.

9.2 Straylight

The Straylight analysis has assumed:

- Surface finish of 4 nm, equivalent to 1% scatter. Yet 2/3 of that scatter leaves through the front.

- Particle scatter 0.1% obscured area, equivalent to 1 year storage in a class 100'000 clean room.
- Inner vane tips: edge radius of 0.05 mm.

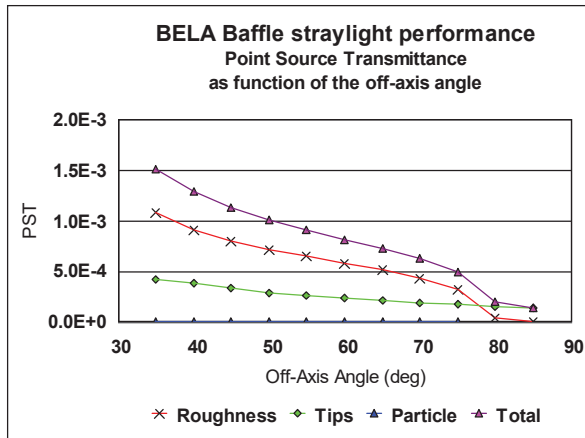


Fig. 13: Straylight performance

According to the latest information about the minimum edge radius of 0.1 mm and a surface finish of 5 nm, the overall PST increases to $2 \cdot 10^{-3}$, i.e. 2 times the target.

9.3 Response to Structure Distortions

Standard CNC manufacturing tolerances have been analysed with magnitudes up to 0.4 mm lateral and 40 μm longitudinal. Some specular stray light was observed, but it stays below the scatter level. The baffle can withstand longitudinal thermal gradients of up to 200 K without occurrence of specular Straylight. Longitudinal gradients of 100K cause 0.7 ~1.9 % additional power trapped mainly at the larger off axis angles. Radial gradients above 40 K cause specular Straylight between $2E-4$ and $4E-4$, yet below the scatter. Radial gradients of 100 K cause additional power absorbed of up to 1.5% mainly at larger of-axis angles.

10. CONTRAVES SPACE ACITVITIES ABOUT MANUFACTURABILITY OF THE BAFFLE

It is foreseen to produce the baffle in several pieces, which will be joined together afterwards (Fig. 14). Except of the flat front vane and the last ellipse, the segments consist of the front facing ellipse and rear facing hyperbola. After the design study, a Contraves Space internally funded development activity has started.



Fig. 14: The baffle and its segments

The primary goal consisted in finding the right process to achieve an rms roughness of 4 nm.

The production steps comprise:

- Rough diamond turning of the outer shape
- Precise diamond turning with a polycrystalline diamond tool of the inner shape
- Hand polishing
- Nickel coating
- Final polishing of the Nickel layer.

For comparison, only the elliptic part was pre-polished and the hyperbolic part was not. After roughness measurement with an atomic force microscope (AFM, Fig. 15) we found that the pre-polished area achieved an rms roughness of 4.1 nm and the not pre-polished area an rms roughness of 8 nm, sufficiently justifying the necessity of pre-polishing

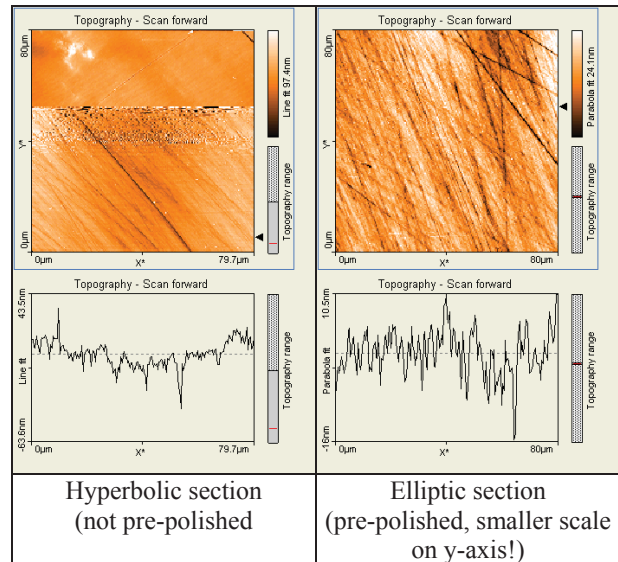


Fig. 15: AFM measurements on elliptic and hyperbolic sections with different polishing grade

Finally, the contour of the segment has been measured on a ZEISS 3D measurement device. The error on circularity resulted with 0.03 mm, which is compliant with the accuracy needed.

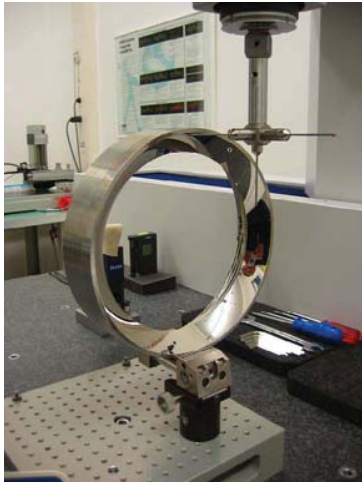


Fig. 15: The finally produced segment during surface shape test on a ZEISS 3D measurement device.

11. CONCLUSIONS

A reflective baffle has been designed according to the Stavroudis concept. It consists of 7 elliptic/hyperbolic segments and will be manufactured by diamond turning in at least 3 pieces. It will be made of aluminium with a wall thickness of 0.5 mm. With the envelope of $\varnothing 298.7\text{mm} \times 362.1\text{ mm}$ length and the fixation bracket it results to a mass of 1.36 Kg. The structure design is compliant with the mechanical loads. The optical performance is limited by the surface properties. The Straylight level reaches twice the target. It will be task of future work to establish an end-to-end Straylight model and to analyse the impact to the payload performance. The power rejection performance almost reached the specification (95%). The assumed surface reflectivity yet requires a UV enhanced silver coating with technological challenges. Moreover, it introduces constraints on the upper temperature. It may be worth to consider a less performing coating (Aluminium), but not having that temperature constraint.

The limiting driver for the upper temperature is not determined so far. The interaction between baffle and the telescope shall be investigated in future works.

The thermal control has been analysed in a first iteration. The average temperatures can be got to reasonable levels around 90°C . Careful control is needed in order to avoid high local temperatures. It is strongly recommended to put emphasis on the determination of the ultimate acceptable average and local temperature levels, including the payload telescope response. This is essential to gain an optimal use of the thermal hardware mass.

12. AKNOWLEDGEMENT

The work presented herein was performed in the frame of the ESA design study "Reflective Baffle for Bepi-Colombo" (ESA contract 18940/05/NL/SFe). We like to thank ESA and their technical officers, Mr. Volker Kirschner and Daniele Stramaccioni, for supporting this activity.

13. REFERENCES

- [1] D. Radovich: "Elliptic Cylindrical Baffle Assembly". US Patent 4,217,026 from 12. Aug. 1980.
- [2] J. C. Bremer: "Baffle design for earth radiation rejection in the cryogenic limb scanning interferometer/radiometer", *SPIE proc.* Vol 245, p. 54-62 (1980), also: *Optical Engineering*, 22(1) p. 166-177 (1983)
- [3] E. Schneider: "Thermal Design of Retro-reflective Stray Light Fore-baffles for Space-borne Optical Systems". *SPIE proc.* Vol 4198 (2001) pp. 82-95
- [4] O. N. Stavroudis, L. D. Foo: "System of reflective telescope baffles" in *Opt. Eng.*, March 1994, Vol. 33 No. 3 p. 675-680
- [5] R. N. Pfisterer, G. L. Peterson: "Dual Reflective Baffle System for the BeCoat Telescope". *SPIE Proc* Vol 1994, p. 112-121., 1994
- [6] W. T. Welford, R. Winston: "*High collection non-imaging optics*". Academic Press, 1989, ISBN 0127428852
- [7] R. Winston, J. C. Miñano, P. Benítez: *Nonimaging Optics*, Elsevier Academic Press 2005, ISBN 0-12-759751-4
- [8] D. Boyd, Hans M. Kuiper: "The compound Parabolic/elliptical Lightshades: Near-Optimal Shading for Cold Radiators". *Proceedings of the 30th International Conference on Environmental Systems (ICES) and 7th European Symposium on Space Environmental Control Systems (2000)*. Article 2000-01-2278.
- [9] W. I. Linlor: "Reflective baffle system with multiple bounces", *SPIE Proc.* Vol. 0675, pp 217-239, 1987.